

Figures 9, 10, 11, 12 and Table 1 corrected

# VORTEX METHOD APPLICATION FOR AERODYNAMIC LOADS ON ROTOR BLADES

Hamidreza Abedi<sup>\*</sup>, Lars Davidson<sup>\*</sup>, Spyros Voutsinas<sup>\*\*</sup>

<sup>\*</sup>(Fluid Dynamics Division, Applied Mechanics Department, Chalmers University of Technology, Göteborg, Sweden)

<sup>\*\*</sup>(Fluid Section, School of Mechanical Engineering, National Technical University of Athens, Athens, Greece)

<sup>\*</sup>e-mail: [abedih@chalmers.se](mailto:abedih@chalmers.se), [lada@chalmers.se](mailto:lada@chalmers.se)

<sup>\*\*</sup>e-mail: [spyros@fluid.mech.ntua.gr](mailto:spyros@fluid.mech.ntua.gr)

## ABSTRACT

Today, wind power is one of the most reliable new energy source serving as an alternative to fossil-fuel generated electricity and is known as widely-distributed clean and renewable energy source. It is now the world's fastest growing energy source and has also become one of the most rapidly expanding industries. The aerodynamics of a wind turbine are governed by the flow around the rotor where the prediction of air loads on rotor blades in different operational conditions and its relation to rotor structural dynamics is crucial for design purposes. Therefore, one of the most important challenges in wind turbine aerodynamics is to predict the forces on the blade accurately where the blade and wake are modeled by different approaches such as Blade Element Momentum (BEM) theory, vortex method and Computational Fluid Dynamics (CFD). In this paper, the application of vortex method for wind turbine aerodynamic performance is used. Different blade models such as lifting line and

lifting surface with prescribed wake model are studied. The main purpose is to find the proper combination of blade and wake model influencing the aerodynamic loads as well as the computational time efficiency. The results of different approaches are compared with the GENUVP code. (See acknowledgements)

Keyword: aerodynamic load, rotor blade, wind turbine, lifting line, lifting surface, panel method, prescribed wake.

## INTRODUCTION

There are different methods to model the aerodynamics of a wind turbine with different level of complexity and accuracy, such as BEM theory and solving the Navier-Stokes equations using CFD. Today, for design purposes, the use of engineering models based on the BEM method prevails. This method is computationally fast and is simply implemented but it is acceptable only for a certain range of flow conditions and breaks down in the turbulent wake state (Hansen [1]). There are some modifications based on empirical corrections to modify the BEM method in order to defeat this restriction. But, they are not relevant to all operating conditions and often go wrong at higher tip speed

ratios (Vermeer [2]). The vortex theory which is based on the potential, inviscid and irrotational flow can be also used to predict aerodynamic performance of wind turbine where the aim is to model a wind turbine consisting of finite number of blades (vs. BEM which assumes a wind turbine as an actuator disk) including the wake geometry. The vortex method has been used for helicopter (Landgrebe [3], Kocurek [4], Egolf [5]) to model the wake and air loads on different operational conditions and for wind turbines (Coton [6], Dumitrescu [7], Kocurek [8]) application as well. According to vortex methods, the trailing and shed vortices originated from the blade, is modeled by either vortex particles or vortex filaments that they move either freely (free wake Gupta [9], Pesmajoglou [10], Voutsinas [11]) or restrictedly by imposing the wake geometry (prescribed wake Chattot [12], Chattot [13]). The prescribed wake requires less computational effort than free wake but it requires experimental data to be valid for a broad range of operating conditions (Curin [14]). The free wake model (Leishman-Bagai [15]) which is the most computationally expensive vortex method is able to predict the wake geometry and loads more accurately than the prescribed wake because of the less restrictive assumptions. Compared to

physical solutions for attached flow conditions with boundary layer corrections and it is also valid over a wider range of turbine operating conditions whereas it is computationally more expensive than the BEM, but it is still feasible as an engineering method. Finally, CFD which solves the Navier-Stokes equations for the flow around the rotor blade is known as the most accurate and expensive method in terms of computational time and it is impractical engineering method for wind turbine application.

## THEORY

Vortex flow theory is based on assuming incompressible ( $\nabla \cdot \mathbf{V} = 0$ ) and irrotational ( $\nabla \times \mathbf{V} = 0$ ) flow at every point except at the origin of the vortex where the velocity is infinite (Anderson [16]). For an irrotational flow, a velocity potential ( $\Phi$ ) can be defined as ( $\mathbf{V} = \nabla \Phi$ ). Therefore, the Laplace's equation ( $\nabla^2 \Phi = 0$ ) can be used (Anderson [16]). In addition, in vortex theory, the vortical structure of the wake can be modeled by either vortex filaments or vortex particles where a vortex filament is modeled as concentrated vortices along an axis with a singularity at the center.

The velocity induced by a straight vortex filament can be determined by the Biot-Savart law as

$$\mathbf{V}_{ind} = \frac{\Gamma}{4\pi} \frac{(r_1 + r_2)(\mathbf{r}_1 \times \mathbf{r}_2)}{r_1 r_2 + \mathbf{r}_1 \cdot \mathbf{r}_2} \quad (1)$$

where  $\Gamma$  is the strength of the vortex filament and  $\mathbf{r}_1, \mathbf{r}_2$  are the distance vectors from the beginning and ending of a vortex segment to an arbitrary point  $P$ , respectively (Anderson [16]). The Biot-Savart law has a singularity when the point of evaluation for induced velocity is located on the vortex filament axis. Also, when the evaluation point is very near to the vortex filament, there is an unphysical large induced velocity at that point. The remedy is either to use a viscous vortex model with finite core size by multiplying a factor to remove the singularity (Leishman-Bagai [15]) or to use a cut-off radius,  $\delta$ . The modified Biot-

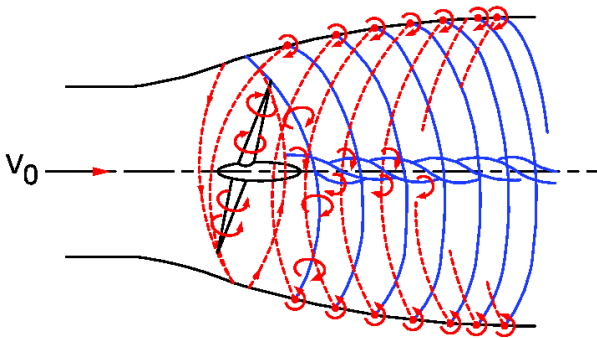


**FIGURE 1.** Schematic of the vortex wake behind the rotor blades (Hansen [1]).

the BEM method, the vortex method is able to provide more

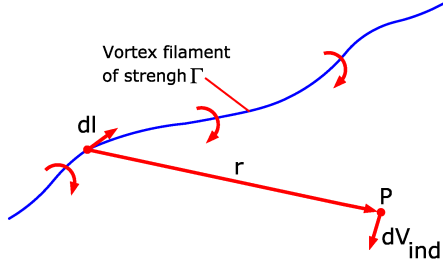


FIGURE 2. Schematic for the Biot-Savart law (Anderson [16]).

Savart law based on the cut-off radius can be written as

$$\mathbf{V}_{ind} = \frac{\Gamma}{4\pi} \frac{(r_1 + r_2)(\mathbf{r}_1 \times \mathbf{r}_2)}{r_1 r_2 + \mathbf{r}_1 \cdot \mathbf{r}_2 + (\delta l_0)^2} \quad (2)$$

where  $l_0$  is the length of the vortex filament. The advantage of the cut-off method is that when the evaluation point moves toward the vortex filament, the induced velocity smoothly goes to zero. A cut-off radius value can be varied between 0.0 and 0.1. It is suggested to use a smaller cut-off value for the blade bound vortex than for the wake. Here,  $\delta$  is set to 0.0001 (Van Garrel [17]).

## Different Approaches

In this paper, three different models are presented: lifting line prescribed wake, lifting surface prescribed wake, panel method prescribed wake. Generally, the blade is modeled by lifting line, lifting surface or lifting panels and the wake can be modeled by either trailing vortices or vortex ring elements.

## Assumptions

Each engineering model is constructed based on some assumptions. Here, some of those are discussed. In prescribed wake model, the upstream flow is uniform, both in time and space, and it is perpendicular to the rotor plane (parallel to the rotating axis). The blade is assumed to be rigid in both models, so the elastic effect of the blade is neglected. The wake is following the helix equation with constant pitch and diameter in the

prescribed wake model, so there is no wake expansion. Since the effect of the induced velocity field by the far wake is small on the rotor blade, the wake extends only to 4 – 5 diameters downstream of the wind turbine rotor plane. The wake elements in the prescribed wake move downstream with a constant velocity including free stream and axial induced velocity. Also, the interaction between the vortex wake filaments is ignored in the prescribed models.

## Lifting Line Prescribed Wake

In this model which is based on the Prandtl lifting line theory, the blade is divided into one or more sections replaced with a straight (for a twisted blade, it is not straight) vortex filament of constant strength  $\Gamma$  (for each section) called bound vortex and the lifting line is located at 1/4 of chord line (downstream the leading edge) along the span (Anderson [16]). The control points storing the bound vortex strength (circulation) and the induced velocity values (generated only by the wake) are located at the bound vortices of each spanwise section. The trailing wake vortices extend downstream from the 1/4 chord making a series of helical horseshoe vortex filaments (see Fig.3). In this approach,

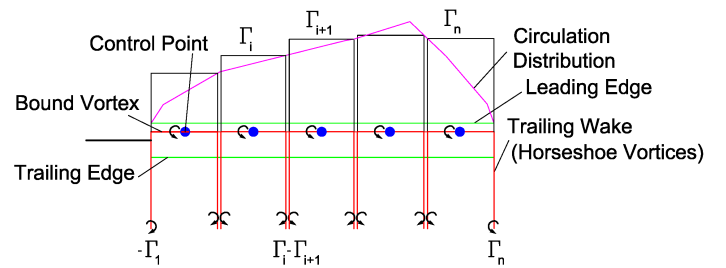
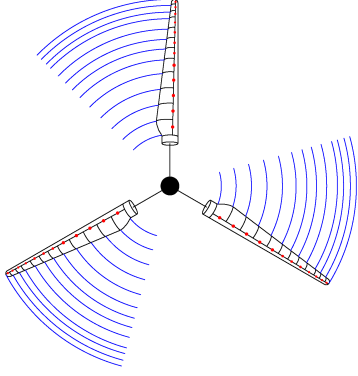


FIGURE 3. Schematic of a blade in lifting line model.

the trailing vortices constructed by vortex filaments originates from the blade bound vortices and emanate from all points along the blade where it makes a helical vortex sheet with constant diameter (Abedi [18]) behind of each rotor blade. This helical

vortex sheet induces velocity field around the rotor blade reducing the angle of attack seen by each blade section. The real an-



**FIGURE 4.** Schematic of prescribed lifting line model.

gle of attack called effective angle of attack can be defined as  $\alpha_{eff} = \alpha_{geom} - \alpha_{ind}$ . Knowing the values of  $\alpha_{eff}$  for each blade section and using the aerodynamic table ( $C_L$ ,  $C_D$  vs.  $\alpha$ ) gives the lift and drag forces per blade span while the torque and power of the wind turbine are then computed by tangential and normal forces with respect to the rotor plane, respectively. In the prescribed wake, an iterative method is used in order to find the final wake geometry, so the solution is started by an initial wake geometry such as a helix and initial bound vortex values in order to determine the strength of the trailing wake vortices. The helix equation is stated as

$$\begin{aligned} x &= r_i \cos(\Omega t + \theta_0) \\ y &= r_i \sin(\Omega t + \theta_0) \\ z &= V_\infty t \end{aligned} \quad (3)$$

where  $r_i$ ,  $\Omega$ ,  $V_\infty$ ,  $\theta_0$  and  $t$  denotes the rotor section radius, rotor blade rotational velocity, free stream velocity, blade initial angle and time, respectively. To initiate the circulation distribution, since each blade section is considered as a 2D airfoil. The Kutta-Jukowski theory ( $L' = \rho V_{rel} \Gamma$ ) is used to calculate the lift force

per span ( $L'$ ) of each blade element where  $\Gamma$  and  $\rho$  denote the circulation and air density, respectively. The lift coefficient is defined as

$$C_L = \frac{L'}{\frac{1}{2} \rho V_{rel}^2 C} \quad (4)$$

where  $L'$ ,  $V_{rel}$  and  $C$  denote the lift per span, the relative velocity and the chord length, respectively. Combining the Kutta-Jukowski theory and Eq.4 gives a correlation for circulation at each blade section as

$$\Gamma = \frac{1}{2} C V_{rel} C_L \quad (5)$$

Note that for the first iteration, the geometric angle of attack is used to compute the lift coefficient whereas for the next iterations, the effective one is used. The trailing vortices are divided into a number of segments and the induced velocity of each wake segments are calculated at the control points located at the blade bound vortex. The vector velocity ( $\mathbf{V}_{rel}$ ) which is the combination of the free stream ( $\mathbf{V}_\infty$ ), rotational ( $\Omega \mathbf{r}$ ) and induced ( $\mathbf{V}_{ind}$ ) velocities at each blade section can then be computed and the modified angle of attack known as effective angle of attack is obtained. Hence, the wake geometry is updated based on the axial ( $V_{ax}$ ) and circumferential ( $\omega$ ) velocities. For example, if the free stream is in the Z direction, then the wake geometry for each section is updated as

$$\begin{aligned} x &= r_i \cos(\omega t + \theta_0) \\ y &= r_i \sin(\omega t + \theta_0) \\ z &= V_{ax} t \end{aligned} \quad (6)$$

where  $V_{ax} = V_\infty + V_{ind,z}$  and  $\omega = \Omega + (V_{ind, circum}/r_i)$ . The effective angle of attack is updated in each iteration changing the lift and drag coefficients as well. By getting the the  $C_L$  and  $C_D$ , the normal and tangential force can be obtained which they are used

to calculate the thrust and power of the wind turbine. This procedure is repeated until the convergency criteria is satisfied. Here the convergency criteria is set based on the generated power so that the power difference between two consecutive iteration is below 0.0001.

### Lifting Surface Prescribed Wake

In the lifting surface model, the blade is divided into a number of panels in span-wise direction and one panel in chord-wise direction (Katz [19]) and the wake can be presented as trailing horseshoe vortices. An iterative method is used in the prescribed

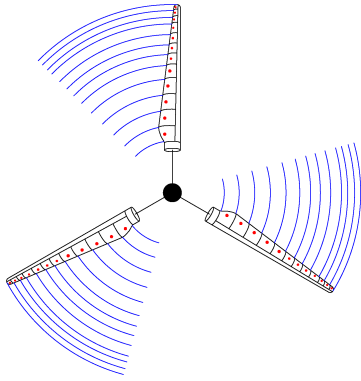


FIGURE 5. Schematic of prescribed lifting surface model.

lifting surface model where, similar to the prescribed lifting line model, an initial wake geometry based on the helix equation (Eq.4) is constructed and it is divided into a number of small segments. A bound vortex is located along the blade at each span-wise section at  $1/4$  chord downstream the leading edge. The strength of each bound vortex  $\Gamma$  is assumed to be constant for the related horseshoe vortex and the positive circulation is defined based on the right-hand rotation rule. The control point of each section where the bound vortices circulation is evaluated, is placed at the  $3/4$  chord behind the leading edge. It is also assumed that the 2D Kutta condition is valid for the 3D model (Katz [19]). In the lifting surface problem, the required

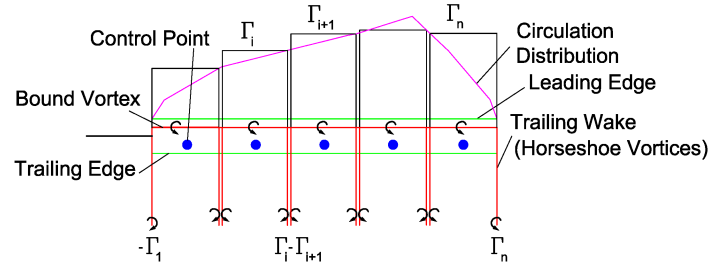


FIGURE 6. Schematic of a blade in lifting surface model.

boundary condition is zero normal flow across the blade surface,  $\nabla(\Phi + \Phi_\infty) \cdot \mathbf{n} = 0$  (Katz [19]). This means that the sum of the wall-normal velocity components at each control point including the induced velocity by the bound and trailing wake vortices as well as the free stream and rotational velocity must be zero, i.e.  $(\mathbf{V}_{ind,bound} + \mathbf{V}_{ind,wake} + \mathbf{V}_\infty + \Omega \mathbf{r}) \cdot \mathbf{n} = 0$ . By applying this equation at each control point on the blade surface, the unknown circulation values  $\Gamma_j$  for each section are determined. Once  $\Gamma_j$  are determined, we are able to compute the induced velocities, the lift and drag distribution over the blade. In order to compute the induced velocity on the blade control points, only the trailing vortices are taken into account. The wake geometry is updated based on the calculated induced velocity similar to Eq.6 and again the new circulation distribution is calculated because of the updated trailing wake geometry. The solution is completed when the convergency criteria is satisfied where again it is set based on the generated power so that the power difference between two consecutive iteration is below 0.0001.

The Kutta-Jukowski theory is used to calculate the potential lift force magnitude of each section as  $L'_j = \rho V_{rel} \Gamma_j$ . By summing the lift force of all sections, the total lift is obtained. By calculating the angle of attack based on the free stream, rotational and induced velocities (only by trailing vortices) and looking up the aerodynamic tables ( $C_L$ ,  $C_D$  vs.  $\alpha$ ) for each blade section, the lift and drag forces are determined resulting in the normal and tangential force on the blades with respect to the rotor plane in

order to compute the power and thrust of the wind turbine.

### Panel Method Prescribed Wake

The panel method is based on the thin lifting surface theory of vortex ring elements (Katz [19]) where the blade surface is replaced by panels which are constructed based on the airfoil camber line of each blade section. The blade surface is divided into a number of panels both in chord-wise and spanwise directions where each panel contains the vortex ring with strength  $\Gamma_{ij}$  in which  $i$  and  $j$  indicate a panel indices in chord wise and spanwise directions, respectively. In order to fulfill the 2D Kutta condition, the leading segment of the vortex ring is located at the 1/4 panel chord line and the control point of each panel is located at the 3/4 panel chord line meaning that the control point is placed at the center of the panel's vortex ring. Also, for satisfying the 3D trailing edge condition for each spanwise section, the strength of the trailing vortex wake rings must be equal to the last vortex ring row in chord wise direction ( $\Gamma_{T.E.} = \Gamma_{Wake}$ ). The normal vector at each control point must be defined in order to apply the zero normal flow boundary condition across the blade (Katz [19]). The trailing wake vortices are modeled as the vortex ring elements which induce the velocity field around the blade (see Fig.8). Similar to the lifting surface model, in order to find

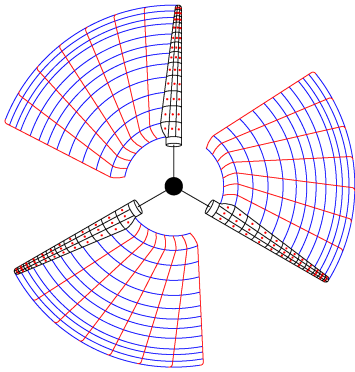


FIGURE 7. Schematic of prescribed panel method.

the strength of each vortex ring element on the blade, a system of equation must be constructed. This can be done by applying the zero normal flow boundary condition at each panel's control point. For a blade with  $M$  spanwise and  $N$  chord wise section, the system of equation is represented as

$$\begin{pmatrix} a_{11} & a_{12} & \cdots & a_{1m} \\ a_{21} & a_{22} & \cdots & a_{2m} \\ \vdots & \vdots & \ddots & \vdots \\ a_{m1} & a_{m2} & \cdots & a_{mm} \end{pmatrix} \begin{pmatrix} \Gamma_1 \\ \Gamma_2 \\ \vdots \\ \Gamma_m \end{pmatrix} = \begin{pmatrix} -(\mathbf{V}_\infty + \boldsymbol{\Omega}\mathbf{r}) \cdot \mathbf{n}_1 \\ -(\mathbf{V}_\infty + \boldsymbol{\Omega}\mathbf{r}) \cdot \mathbf{n}_2 \\ \vdots \\ -(\mathbf{V}_\infty + \boldsymbol{\Omega}\mathbf{r}) \cdot \mathbf{n}_m \end{pmatrix} \quad (7)$$

where  $a_{ij}$  denotes the influence coefficient of the  $j^{th}$  blade vortex ring on the  $i^{th}$  blade control point. Here, the influence coefficient is defined as induced velocity of a vortex ring with strength equal to one on an arbitrary blade control point. Therefore, the influence coefficients of all vortex ring elements (blade surface and wake) on an arbitrary control point are evaluated. This procedure is repeated for all control points of the blade so that  $m = M \times N$ . The solution of the above equation system gives the strength of all vortex ring elements on the blade where the strength of the last vortex ring row determines the wake vortex ring strength. By

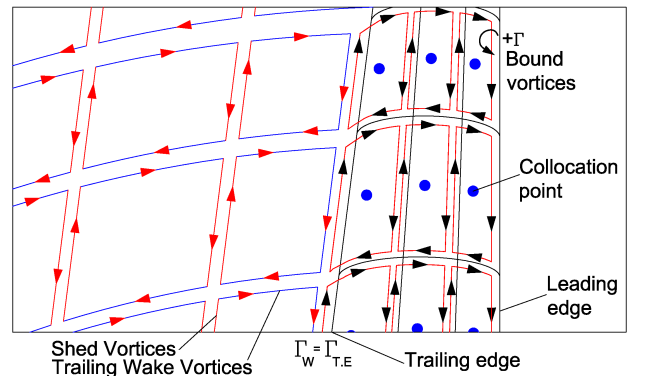


FIGURE 8. Schematic of blade and wake in panel method.

knowing the strength of all vortex ring elements of the blade and the wake, the lift and the induced drag distribution on the blade

is calculated. Again, an iterative method is used by initiation of prescribed wake geometry similar to the previous approaches. The solution of Eq.7 determining the trailing vortex ring wake strength makes it possible to calculate the induced velocity on the blade control points. The induced velocity on the blade changes the wake geometry in each iteration (see Eq.6), so the solution is generally obtained when the difference in the wake geometry between two successive iterations is small. Here the power output is set as the criteria to fulfill the convergency criteria which means that the difference value of calculated power between the two consequent iterations must be lower than 0.0001. The Kutta-Jukowski theorem for each panel gives  $L'_{ij} = \rho V_{rel} (\Gamma_{i,j} - \Gamma_{i-1,j})$ . The effective angle of attack for each section is calculated giving the lift and drag forces by using the aerodynamic tables in order to find the power and thrust of the turbine.

## RESULTS

Here some preliminary results are compared using different approaches. The 5MW reference wind turbine (DOWEC [20]) has been used and the operating condition are  $V_{\infty} = 8.0 [m/s]$  and  $\Omega = 1.0032 [rad/s]$  as free stream and rotational velocity, respectively. The results of each method have been compared with GENUVP (Voutsinas [11]).

Figure 9 shows the geometric and effective angle of attack. As can be seen, in all cases, because of the induced velocity field around the rotor blade, the effective angle of attack is less than the geometric one which makes a significant power reduction of a wind turbine.

The distribution of circulation ( $\Gamma$ ) along the rotor blade is shown in Fig.10 where, as expected, the maximum value occurs near the blade tip.

The tangential and normal forces generating torque and thrust, respectively on a wind turbine are shown in Fig.11 and 12. It is obvious that the maximum value of both tangential and normal forces occurs near the blade tip. This means that the con-

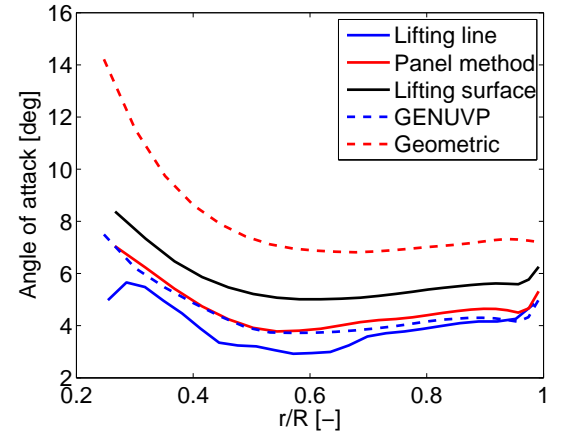


FIGURE 9. Angle of attack, geometric vs. effective

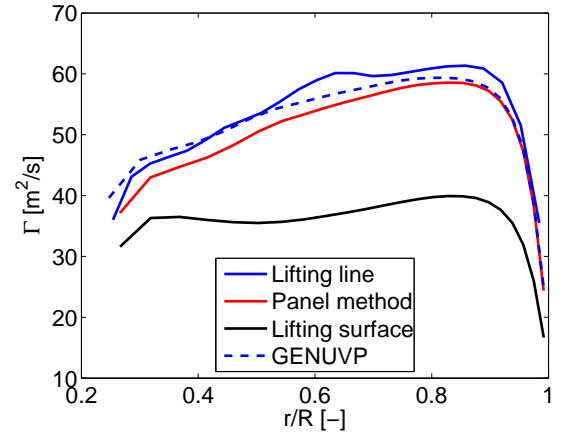
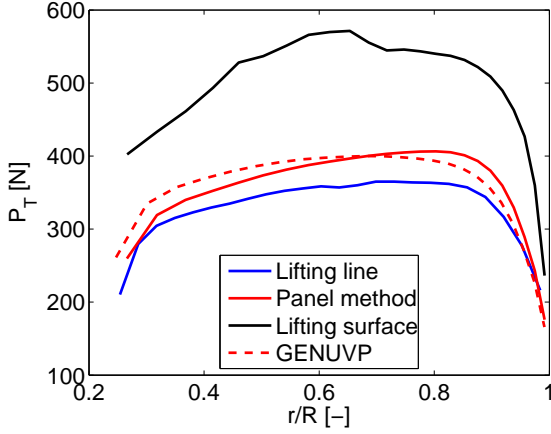


FIGURE 10. Circulation distribution along the blade

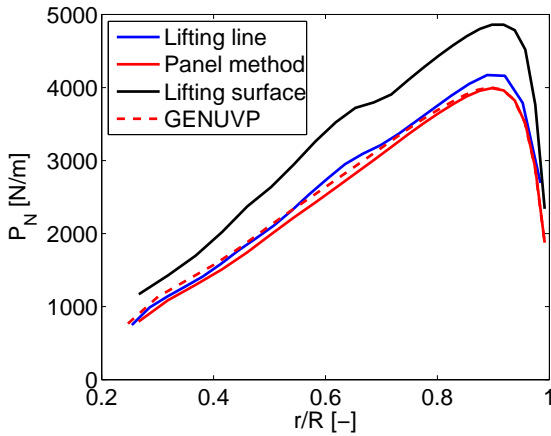
siderable part of the wind turbine power is generated at the blade tip where we expect the strong tip vortex to be located.

Table 1 shows the generated power and the thrust by each model. The computational time based on the 25 blade stations, 6 revolutions and 36 wake elements for each revolution shows that the run time of the prescribed panel method is 35 times more than the prescribed lifting surface model and 2.5 times more than the prescribed lifting line.





**FIGURE 11.** Tangential force acting on the rotor plane



**FIGURE 12.** Normal force acting on the rotor plane

Model	Power [kW]	Thrust [kN]
Lifting line	1819	379
Lifting surface	2780	458
Panel method	2002	360
5MW Ref. (DOWEC [20])	1864	460

**TABLE 1.** Comparison of different approaches

## CONCLUSIONS

Three different approaches of vortex theory application for wind turbine performance analysis were studied. The lifting line model shows good agreement with GENUVP compared with the lifting surface and panel method models. One of the reasons for the different results can be because of the different ways to calculate the circulation distribution along the blade. In the lifting line the values of circulation ( $\Gamma$ ) is obtained by Eq.5 where the properties of each blade section airfoil are considered whereas in the other approaches the circulation values are obtained based on the zero-normal flow boundary condition which means that there is no relation between the blade profile properties and the circulation values.

The method for determination of circulation is very important because it determines the strength of all vortex elements. Hence the induced velocities calculation are strongly dependent on the distribution of circulation along the blade where the combination of free stream, rotational and induced velocities define the velocity field around the rotor blade. The effective angle of attack is calculated based on the  $\alpha_{eff} = \alpha_{geom} - \alpha_{ind}$ , so the small induced velocities make a small induced angle of attack resulting large tangential force and generated power as Fig.11.

In the lifting line, since the vortex wake elements strength is calculated based on the blade airfoil profiles and its computational time is less than the panel method, it is considered as an useful model to study the wake of wind turbine.

In the lifting surface model using only a one panel in chord-wise direction and neglecting the blade surface curvature gives low accuracy. The advantage of this model is the computational time.

In the panel method since the blade is modeled by a number of panels both in chord wise and spanwise directions, it is able to provide detailed load, pressure and velocity distributions over the blade surface compared to other approaches. However, since it is based on the inviscid flow assumption, its accuracy to calcu-



late the forces is low especially when some part of the blade is rotating on the stall condition.

To conclude, the vortex method for analysis of wind turbine aerodynamics can be a suitable way which still needs more comprehensive studies in order to get the more realistic solutions.

## ACKNOWLEDGEMENTS

The technical support of National Technical University of Athens (NTUA) to use the GENUVP is gratefully acknowledged. (GENUVP is an unsteady flow solver based on vortex blob approximations developed for rotor systems by National Technical University of Athens).

This work is a part of the project (Aerodynamic loads on rotor blades) which is financed through the SWPTC (Swedish Wind Power Technology Centre).

## REFERENCES

- [1] Hansen, M. O. L., 2008. *Aerodynamics of Wind Turbines, 2nd edition*. EarthScan.
- [2] Vermeer, L. J., Sørensen, J. N., and Crespo, A., 2003. "Wind Turbine Wake Aerodynamics". *Prog. in Aerospace Sciences*, **39**, pp. 467–510.
- [3] Landgrebe, A., 1972. "The wake geometry of a hovering rotor and its influence on rotor performance". *Journal of the American Helicopter Society*, **17**, No. 4, pp. 2–15.
- [4] Kocurek, J. D., and Tangler, J. L., 1977. "A prescribed wake lifting surface hover performance analysis". *Journal of the American Helicopter Society*, **22**, No. 1, pp. 24–35.
- [5] Egolf, T. A., and Landgrebe, A. J., 1983. "Helicopter rotor wake geometry and its influence in forward flight, vol. 1 generalized wake geometry and wake effects in rotor airloads and performance". *NASA CR-3726*.
- [6] Coton, F. N., and Wang, T., 1999. "The prediction of horizontal axis wind turbine performance in yawed flow using an unsteady prescribed wake model". *Journal of Power and Energy*, **213**, pp. 33–43.
- [7] Dumitrescu, H., and Cardos, V., 1999. "Wind turbine aerodynamic performance by lifting line method". *International Journal of Rotating Machinery*, **4**, No. 1, pp. 141–149.
- [8] Kocurek, D., 1987. "Lifting surface performance analysis for horizontal axis wind turbines". *SER/STR-217-3163*.
- [9] Gupta, S., 2006. *Development of a time-accurate viscous Lagrangian vortex wake model for wind turbine applications*. University of Maryland, Department of Aerospace Engineering.
- [10] Pesmajoglou, S., and Graham, J., 2000. "Prediction of aerodynamic forces on horizontal axis wind turbines in free yaw and turbulence". *Journal of Wind Engineering and Industrial Aerodynamics*, **86**, pp. 1–14.
- [11] Voutsinas, S., 2006. "Vortex methods in aeronautics: how to make things work". *International Journal of Computational Fluid Dynamics*, **20**, pp. 3–18.
- [12] Chattot, J., 2007. "Helicoidal vortex model for wind turbine aeroelastic simulation". *Computers and Structures*, **85**, pp. 1072–1079.
- [13] Chattot, J., 2003. "Optimization of wind turbines using helicoidal vortex model". *Journal of Solar Energy Engineering*, **125**, pp. 418–424.
- [14] Curin, H., Coton, F., and Wood, B., 2008. "Dynamic prescribed vortex wake model for AERODYN/FAST". *Journal of Solar Energy Engineering*, **130**.
- [15] Gordon Leishman, J., and Mahendra J. Bhagwat Ashish Bagai, 2002. "Free vortex filament methods for the analysis of helicopter rotor wakes". *Journal of Aircraft*, **39**.
- [16] Anderson, J. D., 2001. *Fundamentals of Aerodynamics*, 3rd ed. McGraw-Hill.
- [17] van Garrel, A., August 2003. *Development of a wind turbine aerodynamics simulation module*. ECN report, ECN-

C-03-079.

- [18] Abedi, H., 2011. *Aerodynamic Loads On Rotor Blades*. Department of Applied Mechanics, Division of Fluid Dynamics, Chalmers University of Technology.
- [19] Katz, J., and Allen Plotkin, 2001. *Low-Speed Aerodynamics*, 2nd ed. Cambridge University Press.
- [20] Jonkman, J., Butterfield, S., Musial, W., and Scott, G., 2009, NREL/TP-500-38060. *Definition of a 5-MW reference wind turbine for offshore system development*. National Renewable Energy Laboratory, Colorado, USA.